

Fabrication of polymer microsphere-based whispering gallery mode microcavities of various sizes incorporating Ag-In-S quantum dots

© S.A. Khorkina¹, A.P. Tkach¹, K.A. Maleeva¹, K.V. Bogdanov^{1,¶}

¹ International research and educational center for physics of nanostructures, ITMO University, Saint-Petersburg, Russia

¶-mail: kirw.bog@gmail.com

Received May 02, 2024

Revised May 13, 2024

Accepted May 13, 2024

The presented methodology describes the fabrication of active spherical microresonator structures with whispering gallery modes, based on polystyrene microspheres and AgInS₂ quantum dots. These microresonators were obtained through electrostatic layer-by-layer deposition in aqueous suspensions. The ability to precisely tune the luminescent response of the active microresonators by adjusting the size of the polystyrene microsphere template is demonstrated. This size-dependent tunability of the optical properties makes these structures highly promising for integration into sensor devices, where optimized performance can be achieved through tailored resonator design.

Keywords: whispering gallery modes, quantum dots, layer-by-layer deposition, microresonators.

DOI: 10.61011/EOS.2024.05.59115.6464-24

Introduction

Creation and improvement of resonators capable of confining a light wave within a material are of great interest in applications such as sensor platforms, low-threshold stimulated emission sources, optical filters, interferometers, waveguides, etc. [1–5]. Whispering gallery mode (WGM) resonators are one of the most promising optical technology areas. Such resonators have a set of unique properties such as high sensitivity to environment, high detection limits. WGM resonators may be divided into two types: active and passive. Passive resonators are made of an unalloyed material, therefore their application is limited due to difficulty in excitation radiation supply and to a complex-geometry evanescent wave coupler [6]. Alternatively, active resonators may be excited in free space and, thus, facilitate remote excitation of structures [2]. However, application of active resonators is essentially limited by the properties of an amplifying medium, including uncontrolled spectral detection range [7]; temporal instability of organic dyes [8,9]; toxicity of heavy metals (Cd-, Hg- and Pb-based structures) [10–12]. Low-toxic semiconductor AgInS₂ quantum dots (QD) with unique optical and electronic properties are a promising material offering new opportunities in the development of active WGM resonators.

One of the main areas for improvement of the technique for creating active resonators is the involvement of various amplifying media: organic dyes, perovskite nanocrystals, carbon dots and QDs with various composition. Organic dyes and perovskites usually provide high photoluminescence quantum yield (PLQY), but they lack temporal stability and photostability that are necessary for long-term operation of the WGM resonator. II-VI quantum dots (Cd, Hg and Pb chalcogenides) are generally stable, but toxic heavy elements existing in these nanoparticles almost preclude from using them in biosciences or for any

end user. To avoid the constraints of materials that are currently used, we propose ternary quantum dots free of toxic metals, i.e. AgInS₂/ZnS (AIS) QDs with bright and tunable radiation spectrum. AIS quantum dots have optical properties suitable for bioimaging, nonlinear optical devices and sensoric applications [13–15]. Position of their PL band peak may be adjusted from green to near infrared optical spectrum range depending on stoichiometry and particle size, which provides high flexibility of the obtained active resonators. Meanwhile, high photostability [16], long lifetimes (hundreds of nanoseconds) [17] and high PL quantum yield (up to 90%) [18] make AIS QDs optimum candidates for amplifying medium in active WGM resonators.

Microspheres are the most suitable geometry for implementing the WGM effect due to their capability of effective light confinement and precision control of resonant modes. Microspheres used as a base platform for active WGM resonators make it possible to achieve high quality and compatibility with various materials. Previous studies have shown that CdSe QDs were mostly used for deposition onto microspheres during WGM generation [12,19–22]. The main methods for introducing QDs into a resonator are swelling and layer-by-layer deposition whereby the latter is preferable for fabrication of active microcavities due to their ability to control precisely the layer thickness and composition leading to more homogeneous structure and layer-by-layer fabrication. Study [12] shows successful application of the layer-by-layer deposition method for creating tunable WGM radiation by adsorption of thin polyelectrolyte layers on the surface of a silica microsphere with integrated CdSe QDs. The influence of the QD layer thickness on the parameters and position of WGM resonance variations has been in turn studied in [20]. However, investigations of the influence of the resonator base platform dimensions on the parameters of the active magnetostriction resonance

are not complete with respect to morphological features of this type of resonator platform. This is in turn particularly interesting area of investigation because the dependence of the resonator base dimensions is an important factor for investigating the WGM generation, and future research in this field may provide valuable information about the fundamental physics of processes taking place in the active WGM resonators and potential applications of such systems.

Materials and methods

Reagents

Polymer microspheres made of polystyrene with COOH charge/groups on the surface (PMS) with a size of 3, 4, 5, 6 μm were provided by Polymer Latex (Saint Petersburg, Russia), polyallylamine hydrochloride (PAH) (molecular weight ~ 50000) was bought from Sigma Aldrich and used without additional purification, sodium chloride (C.P.) was bought from LenReaktiv, indium chloride tetrahydrate (III) ($\text{InCl}_3 \cdot 4\text{H}_2\text{O}$), silver nitrate (AgNO_3), zinc acetate dihydrate (II) ($\text{Zn}(\text{CH}_3\text{COO})_2 \cdot 2\text{H}_2\text{O}$), sodium sulfide nonahydrate ($\text{Na}_2\text{S} \cdot 9\text{H}_2\text{O}$), sodium chloride (NaCl), ammonium hydroxide solution ($\text{NH}_3 \cdot \text{H}_2\text{O}$), thioglycolic acid (TGA), isopropanol, acetone, distilled water.

Ag-In-S QD synthesis

Colloidal AgInS_2 quantum dots with ZnS shell were synthesized using the adapted method described in [16]. First, solution with AgNO_3 , TGA and ammonia alkali was prepared, then InCl_3 and Na_2S were added. After heating and adding TGA and $\text{Zn}(\text{CH}_3\text{COO})_2$ solutions, the ZnS shell was grown. After completion of the synthesis process, the prepared solution was washed with the isopropanol and acetone mixture to remove reaction by-products and ligands remaining in excess. Purified AIS/ZnS QDs (hereinafter referred to as AIS) were diluted in deionized water and stored in a refrigerator.

Fabrication of active microcavities

Active WGM microcavities are fabricated from polymer microspheres that have a negative charge ($\xi \approx -45 \text{ mV}$) on the surface due to functionalization with carboxyl groups. The study used PMS with different diameters of 3, 4, 5 and 6 μm . Ternary AIS quantum dots obtained using the protocol described in [23] served as the active medium in the resonators. Fabrication process of the active microcavities is identical for PMS with different diameters and is shown in Figure 1. The microsphere is coated with PAH that provides a positive surface charge ($\xi \approx +44 \text{ mV}$). For this, PAH and PMS were mixed in 1 M sodium chloride solution, then washed three times in distilled water: centrifuging and decantation of supernatant liquid, adding water, shaking. Concentrated AIS aqueous solution was added to PAH-coated PMS, the mixture was

shaken during 24 h. The obtained active microcavities were washed to remove excess AIS in the aqueous solution using the same procedure as for PMS+PAH.

Instruments and active microcavity investigation methods

WGM spectra of active microcavities were recorded using Renishaw InVia Raman microspectrometer (Renishaw, UK) with 488 nm Ar^+ -laser. The spectrometer has a back-scatter geometry with 50 \times Leica ($\text{NA} = 0.78$) lens.

SEM images of microcavities for monitoring uniform deposition of AIS onto PMS were obtained using Merlin-Zeiss electron microscope at 15 kV and a cathode current $of I = 5000 \text{ pA}$. Oxford XMax 80 energy-dispersive analysis module and Aztec software were used for the elemental analysis.

Stability of the obtained structures was examined and deposition uniformity was monitored through changing the surface charge (ξ -potential) using Zetasizer Nano (Malvern, UK).

Luminescent-microscopic images of PMS were made using LSM 710 confocal laser scanning microscope (Carl Zeiss, Germany) on the basis of Axio Imager Z1 wide-field microscope with EC Epiplan-Apochromat 50 \times ($\text{NA} = 0.95$) lens. Photoluminescence was induced by a 405 nm diode laser and collected by QUASAR 32-channel spectral detector integrated into the microscope system.

Results and discussions

Optical properties of polystyrene microspheres and Ag-In-S quantum dots were investigated using the fluorescence microscopy and scanning electron microscopy (SEM) methods. The image of PMS with AIS/ZnS QDs on the surface obtained using the fluorescence microscopy is shown in Figure 2, *a* demonstrating the functionalized microspheres with enhanced luminescence on the periphery. Ag-In-S quantum dots are uniformly distributed on the surface and have intense visible-range photoluminescence, which is indicative of their potential use as an amplification and detection source or microspheres. Examination of microcavities using the scanning microscope (Figure 2, *b*) shows that the microsphere surface is characterized by smoothness and sphericity supporting successful fabrication and high quality of functional microstructures.

In WGM-effect optical resonators, light waves are propagated at particular reflection angles leading to resonance enhancement of radiation. This effect results from repeated reflections of light waves from inner surfaces of the resonators and by light wave interference inducing two sets of modes with orthogonal polarization: transverse electric (TE) mode and transverse magnetic (TM) mode [24]. WGM resonators have special properties such as high degree of coherency and capability of monitoring their resonance characteristics. Figure 3 shows schematic diagram of the resonance process in a WGM resonator using geometrical

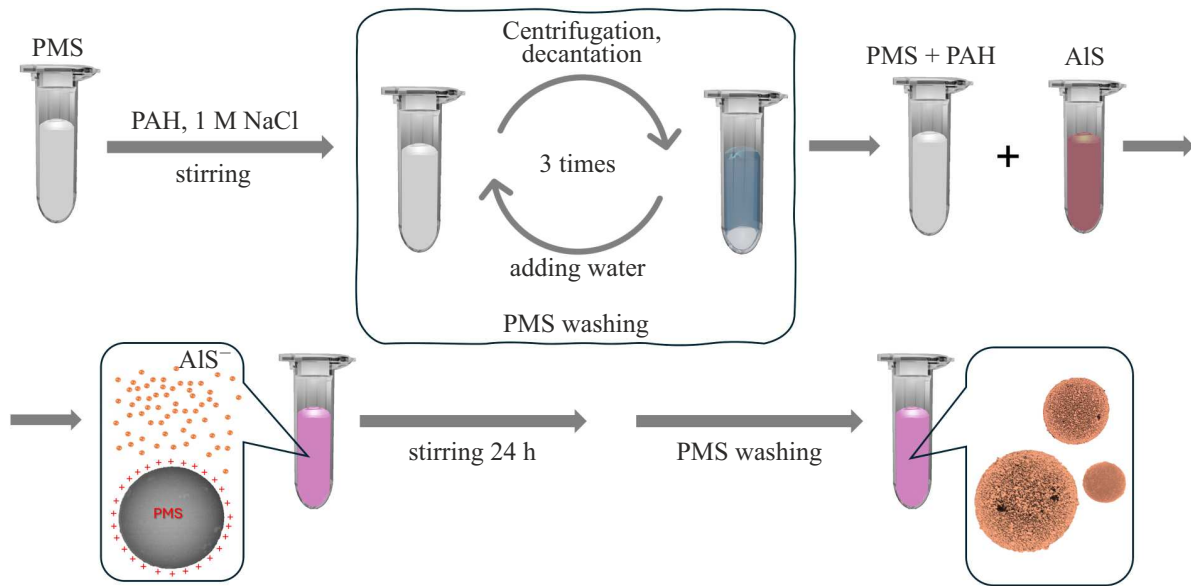


Figure 1. Flow chart of fabrication of active microcavities using polymer microspheres and AIS.

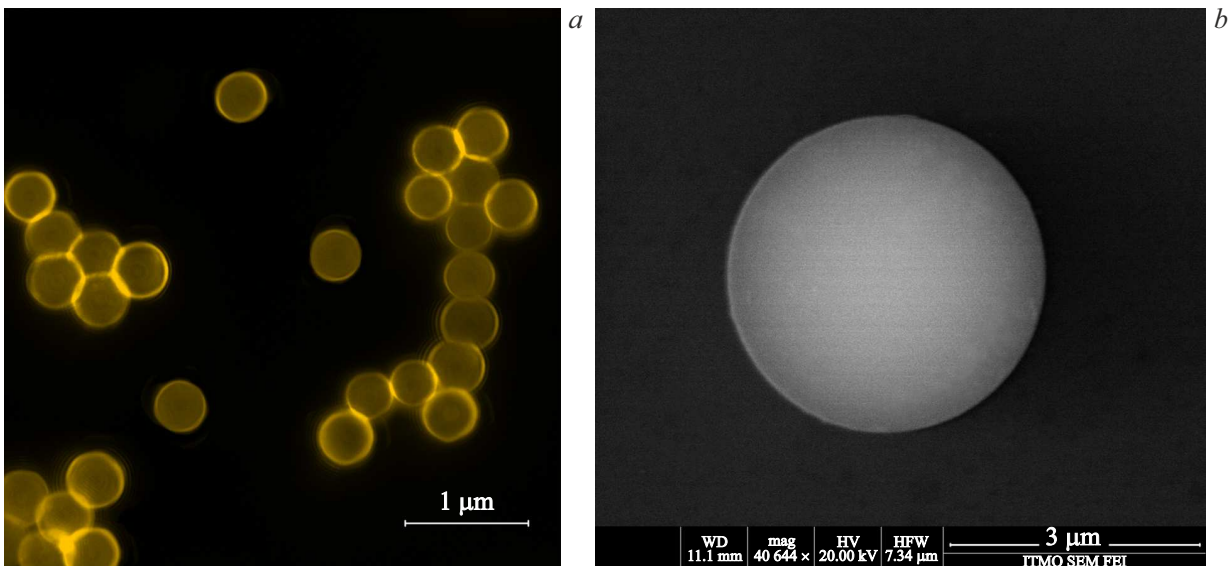


Figure 2. (a) pseudocolor images of PMS with QDs obtained using fluorescence microscopy; (b) SEM image of a single microsphere.

and wave optics approximations. Typical PL spectra for microcavities with different dimensions of the base platform demonstrate a series of closely spaced periodic peaks corresponding to different WGM resonances. Each mode represents a particular wavelength at which the system can effectively store the energy for a long time. Spectra of microcavities with various dimensions differ from each other by several parameters. Increase in the microsphere diameter leads to the growth of the number of observed resonant states in one spectral range. This dependence results from the decrease in the distance between the neighboring modes and the increase in the mode number, which leads to the decrease in the free spectral range (FSR). WGM spectra are shown after normalization and subtraction of Raman

scattering bands of polystyrene in Figure 4. Before the analysis of structure, modes were identified by their polar numbers. According to the explicit asymptotic equation derived by Lam et al., positions of modes with mode number l and sequence number i may be obtained as follows [25]:

$$nx_{l,i} = v + 2^{-\frac{1}{3}} \alpha_i v^{\frac{1}{3}} - \frac{P}{(n^2 - 1)^{\frac{1}{2}}} + \left(\frac{3}{10} 2^{-\frac{2}{3}} \right) \alpha_i^2 v^{-\frac{1}{3}} - \frac{2^{-\frac{1}{3}} P (n^2 - \frac{2P^2}{3})}{(n^2 - 1)^{\frac{3}{2}}} \alpha_i v^{-\frac{2}{3}} + O(v^{-1}), \quad (1)$$

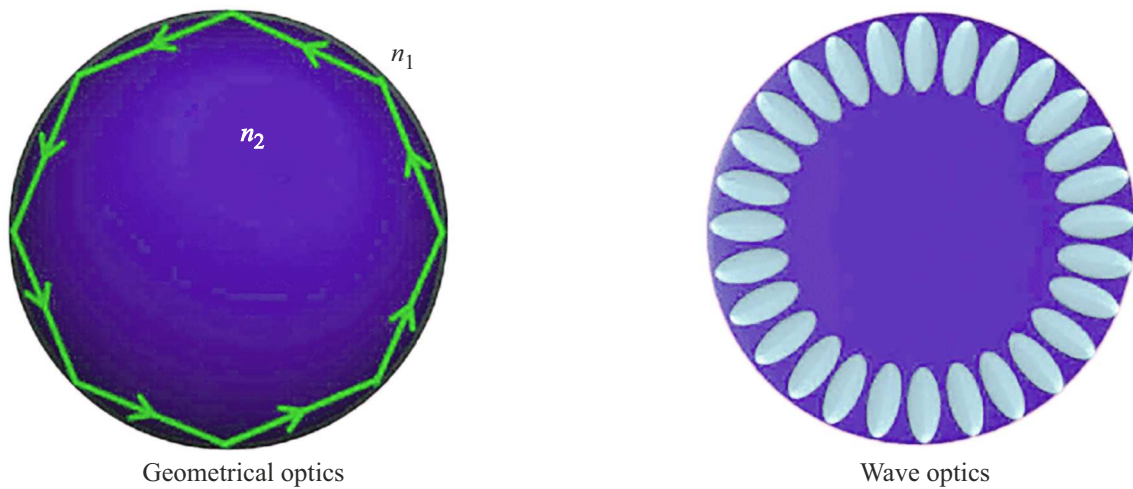


Figure 3. Schematic diagram showing the resonance of the spherical WGM microcavity using geometrical and wave optics. n_1 and n_2 — are the refractive indices of the corresponding media. Small ellipsoids represent the resonant mode distribution in electric field.

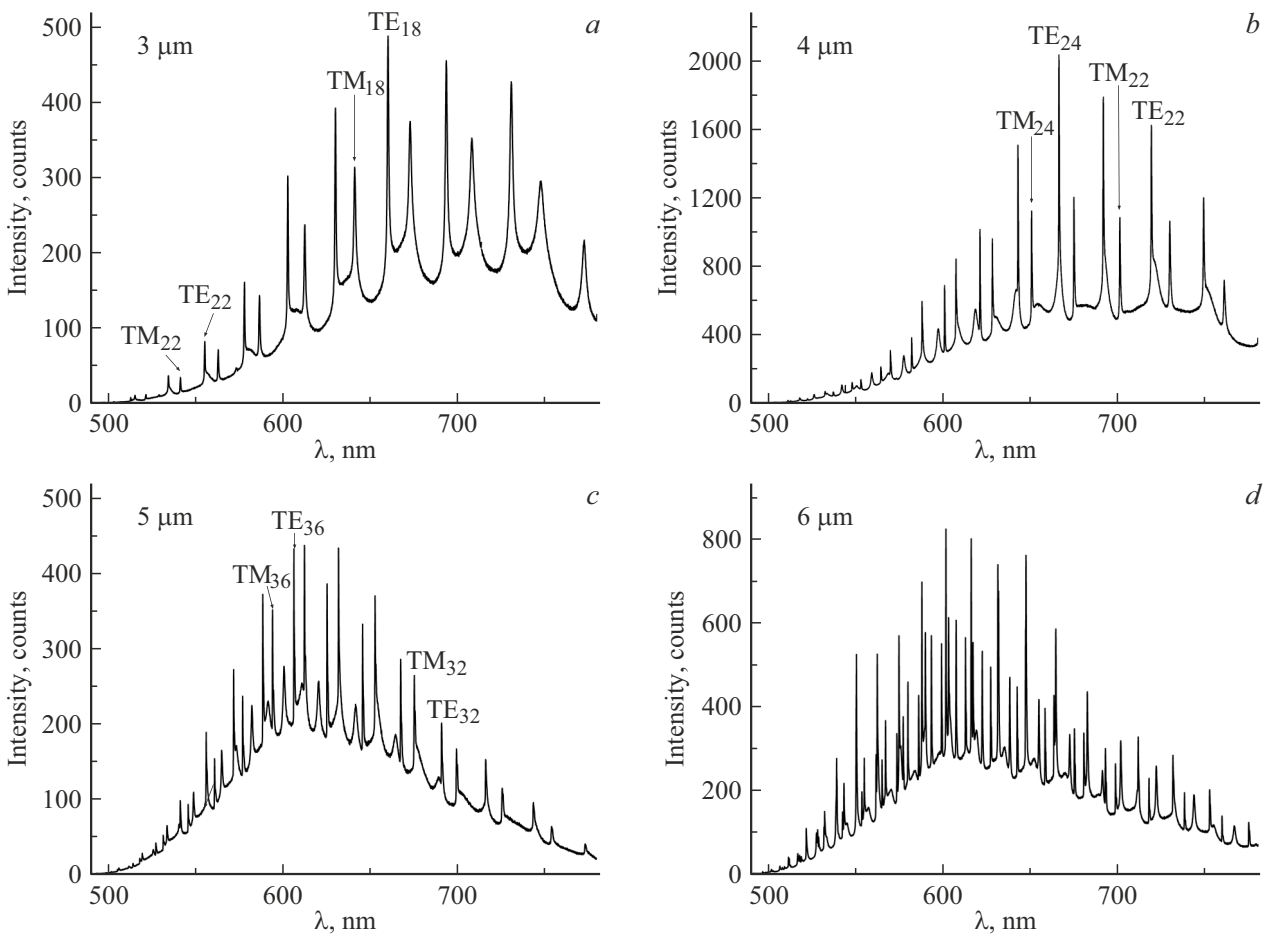


Figure 4. WGM spectra of microcavities with different polymer sphere diameters: (a) $3\ \mu\text{m}$, (b) $4\ \mu\text{m}$, (c) $5\ \mu\text{m}$, (d) $6\ \mu\text{m}$ — positions of some modes are also indicated.

where $x_{l,i} = 2\pi a/\lambda$ is a dimensionless parameter, a is the microsphere radius, n is the refractive index of the resonator material, $P = n$ for the TE-mode and $P = 1/2$ for the TM-mode, α_i — i -th root of the Airy function, $v = l + 1/2$.

In this study, $\alpha_1 = 2.338$ for $i = 1$ and $\alpha_2 = 4.088$ for $i = 2$. refractive index dispersion of polystyrene was considered by calculation of particular wavelength-dependent values using the experimental data from [26]. Another

WGM resonator parameters for different microsphere sizes

Diameter of sphere, μm	TE-mode number	Q factor	FSR, nm
3	18	900	19
4	25	1600	15
5	36	2300	12
6	42	3100	9

important aspect to be considered is how the amplifying medium properties influence the resonance quality. Q -factor is used to evaluate the total energy stored in the resonator with respect of the loss of energy [27]. Q factor for a particular mode was calculated using the following equation:

$$Q = \lambda / \Delta\lambda, \quad (2)$$

where λ and $\Delta\lambda$ are the wavelength and resonance peak full width at half maximum, respectively. The higher Q factor the longer oscillations are retained in the system. The table contains Q factors and FSR for microcavities with different sizes depending on the TE-mode number.

The number of light reflections in the sphere cross-section increases as the optical path length increases. This demonstrates that the modes recorded on microcavities with large diameters have a higher number (Figure 4), therefore, the free spectral range decreases. Moreover, more detailed examination shows that FSR between modes with the same numbers in microcavities with different sizes does not coincide. For example, the distance between TE_{22} and TM_{22} is larger in the microcavity with a diameter of $4\mu\text{m}$ compared with the microcavity with a diameter of $3\mu\text{m}$, and the distance between the doublets containing TE- and TM-modes with the same numbers grows as the microcavity size increases (Figure 5). Such variations of microcavity mode positions are also observed for smaller size distributions and on other luminescent media [28]. These results are indicative of a complex dependence of microcavity spectra on microcavity sizes and mode parameters.

Conclusions

The study has established that the resonator sizes have significant influence on the Q factor and number of generated modes. The described technique for fabricating active microcavities is used for fine tuning their PL characteristics, thus, providing good prospects for application in sensor devices and creation of unclonable functions. It has been shown that large resonator sizes lead to the highest Q factor up to ~ 3000 . On the contrary, small sizes have a small number of generated resonant modes in the investigated spectral range and have low Q factor. It has been established experimentally that for larger microspheres the number of generated modes is larger which is attributed

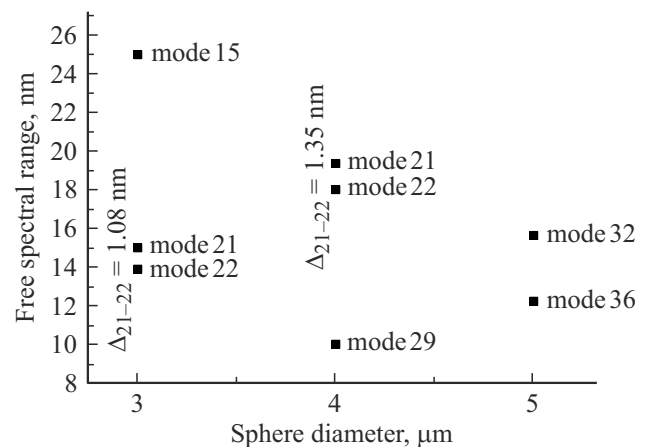


Figure 5. Free spectral range for TM- and TE-modes with the same number on spheres with different diameters. The difference (Δ) between the neighboring doublets of modes 21 and 22 on $3\mu\text{m}$ and $4\mu\text{m}$ spheres is also indicated.

to the principle of an integer number of wavelengths for rereflection. The study describes the technique for creating active spherical microcavity structures with the whispering gallery modes using polystyrene microspheres and AgInS_2 quantum dots. Possibilities of precise tuning of luminescent response of the active microcavities by varying the resonator base size have been investigated. This streamlining facilitates efficient utilization of data structures in sensor devices to achieve optimum characteristics.

Funding

This study was funded by the Russian Science Foundation (Contract 23-72-10010).

Conflict of interest

The authors declare that they have no conflict of interest.

References

- [1] N. Toropov, G. Cabello, M.P. Serrano, R.R. Gutha, M. Rafti, F. Vollmer. *Light Sci. Appl.*, **10** (1), 42 (2021). DOI: 10.1038/s41377-021-00471-3
- [2] D. Venkatakrishnarao, E.A. Mamonov, T.V. Murzina, R. Chandrasekar. *Adv. Opt. Mater.*, **6** (18), (2018). DOI: 10.1002/adom.201800343
- [3] K.J. Vahala, *Nature*, **424** (6950), 839–846 (2003). DOI: 10.1038/nature01939
- [4] D.M. Beggs, M.A. Kaliteevski, S. Brand, R.A. Abram, *J. Mod. Opt.*, **51** (3), 437–446 (2004). DOI: 10.1080/09500340408235535
- [5] F.Q. Mohammed, T.S. Mansoor, A.W. Abdulwahhab. *Photonic Netw. Commun.*, **38** (2), 270–279 (2019). DOI: 10.1007/s11107-019-00855-x
- [6] Y. Zhang, Q. Song, D. Zhao, X. Tang, Y. Zhang, Z. Liu, L. Yuan. *Opt. Laser Technol.*, **159** 108955 (2023). DOI: 10.1016/j.optlastec.2022.108955

- [7] A. Cholasettyhalli Dakshinamurthy, T.K. Das, P. Ilaiyaraja, C. Sudakar. *Front. Mater.*, **6** (2019). DOI: 10.3389/fmats.2019.00282
- [8] X. Wang, H. Li, Y. Wu, Z. Xu, H. Fu. *J. Am. Chem. Soc.*, **136** (47), 16602–16608 (2014). DOI: 10.1021/ja5088503
- [9] J. Zhao, Y. Yan, C. Wei, W. Zhang, Z. Gao, Y.S. Zhao. *Nano Lett.*, **18** (2), 1241–1245 (2018). DOI: 10.1021/acs.nanolett.7b04834
- [10] Z. Liu, J. Yang, J. Du, Z. Hu, T. Shi, Z. Zhang, Y. Liu, X. Tang, Y. Leng, R. Li. *ACS Nano*, **12** (6), 5923–5931 (2018). DOI: 10.1021/acsnano.8b02143
- [11] S.I. Shopova, G. Farca, A.T. Rosenberger, W.M.S. Wickramanayake, N.A. Kotov, *Appl. Phys. Lett.*, **85** (25), 6101–6103 (2004). DOI: 10.1063/1.1841459
- [12] D.E. Gómez, I. Pastoriza-Santos, P. Mulvaney. *Small*, **1** (2), 238–241 (2005). DOI: 10.1002/sml.200400019
- [13] S.R. Thomas, C.-W. Chen, M. Date, Y.-C. Wang, H.-W. Tsai, Z.M. Wang, Y.-L. Chueh. *RSC Adv.*, **6** (65), 60643–60656 (2016). DOI: 10.1039/C6RA05502H
- [14] H. Zhong, Z. Bai, B. Zou. *J. Phys. Chem. Lett.*, **3** (21), 3167–3175 (2012). DOI: 10.1021/jz301345x
- [15] W.M. Girma, M.Z. Fahmi, A. Permadi, M.A. Abate, J.-Y. Chang. *J. Mater. Chem. B*, **5** (31), 6193–6216 (2017). DOI: 10.1039/C7TB01156C
- [16] A. Raevskaya, V. Lesnyak, D. Haubold, V. Dzhagan, O. Stroyuk, N. Gaponik, D.R.T. Zahn, A. Eychmüller. *J. Phys. Chem. C*, **121** (16), 9032–9042 (2017). DOI: 10.1021/acs.jpcc.7b00849
- [17] V. Kuznetsova, A. Tkach, S. Cherevko, A. Sokolova, Y. Gromova, V. Osipova, M. Baranov, V. Ugolkov, A. Fedorov, A. Baranov. *Nanomaterials*, **10** (8), 1569 (2020). DOI: 10.3390/nano10081569
- [18] M.D. Regulacio, K.Y. Win, S.L. Lo, S.-Y. Zhang, X. Zhang, S. Wang, M.-Y. Han, Y. Zheng. *Nanoscale*, **5** (6), 2322 (2013). DOI: 10.1039/c3nr34159c
- [19] H.T. Beier, G.L. Coté, K.E. Meissner. *Ann. Biomed. Eng.*, **37** (10), 1974–1983 (2009). DOI: 10.1007/s10439-009-9713-2
- [20] H.T. Beier, G.L. Coté, K.E. Meissner. *J. Opt. Soc. Am. B*, **27** (3), 536 (2010). DOI: 10.1364/JOSAB.27.000536
- [21] S. Pang, R.E. Beckham, K.E. Meissner. *Appl. Phys. Lett.*, **92** (22), (2008). DOI: 10.1063/1.2937209
- [22] M. Charlebois, A. Paquet, L.S. Verret, K. Boissinot, M. Boissinot, M.G. Bergeron, C.N. Allen. *Nanoscale Res. Lett.*, **5** (3), 524–532 (2010). DOI: 10.1007/s11671-010-9541-1
- [23] V. Kuznetsova, V. Osipova, A. Tkach, M. Miropoltsev, D. Kurshanov, A. Sokolova, S. Cherevko, V. Zakharov, A. Fedorov, A. Baranov et al. *Nanomaterials*, **11** (1), 109 (2021). DOI: 10.3390/nano11010109
- [24] A. Chiasera, Y. Dumeige, P. Féron, M. Ferrari, Y. Jestin, G. Nunzi Conti, S. Pelli, S. Soria, G.C. Righini. *Laser Photon. Rev.*, **4** (3), 457–482 (2010). DOI: 10.1002/lpor.200910016
- [25] C.C. Lam, P.T. Leung, K. Young. *J. Opt. Soc. Am. B*, **9** (9), 1585 (1992). DOI: 10.1364/JOSAB.9.001585
- [26] N. Sultanova, S. Kasarova, I. Nikolov. *Acta Phys. Pol. A*, **116** (4), 585–587 (2009). DOI: 10.12693/APhysPolA.116.585
- [27] W.W. Wong, C. Jagadish, H.H. Tan. *IEEE J. Quantum Electron.*, **58** (4), 1–18 (2022). DOI: 10.1109/JQE.2022.3151082
- [28] S.A. Grudinkin, A.A. Dontsov, N.A. Feoktistov, M.A. Baranov, K.V. Bogdanov, N.S. Averkiev, V.G. Golubev. *Semiconductors*, **49** (10), 1369–1374 (2015). DOI: 10.1134/S1063782615100085

Translated by E.Illinskaya